4762 *Chem. Mater.* **2010,** *22,* 4762–4768
DOI:10.1021/cm101654q

CHEMISTRY OF MATERIALS
Article

Effect of the Phobic Segregation between Fluorinated and Perhydrogenated Chains on the Supramolecular Organization in Ionic Aromatic Dendrimers

Silvia Hernández-Ainsa,[†] Joaquín Barberá,*[,†] Mercedes Marcos,[†] and José Luis Serrano[‡]

[†]*Departamento de Química Orgánica, Facultad de Ciencias-Instituto de Ciencia de Materiales de Aragón, Universidad de Zaragoza-CSIC, C/Pedro Cerbuna 12, 50009-Zaragoza (Spain), and*
[‡]*Instituto de Nanociencia de Aragón, Universidad de Zaragoza, Pedro Cerbuna 12, 50009-Zaragoza (Spain)*

Received June 14, 2010. Revised Manuscript Received July 14, 2010

Two novel series of codendrimers constituted by the grafting of poly(propylene imine) PPI-$(NH_2)_{16}$ ($G = 3$) with aromatic acids substituted with fluorinated and perhydrogenated chains in different proportions have been synthesized and their liquid crystalline properties have been investigated. Series I is generated by the ionic attachment of 4-decyloxybenzoic acid and 4-(1H,1H,2H,2H)-perfluorodecyloxybenzoic acid in different proportions. Series II results from the ionic junction of eight units of 3,4-didecyloxybenzoic acid or 3,4,5-tridecyloxybenzoic acid and eight units of 4-decyloxybenzoic acid or 4-(1H,1H,2H,2H)-perfluorodecyloxybenzoic acid. The liquid crystalline behavior has been investigated by means of differential scanning calorimetry (DSC), polarizing optical microscopy (POM), and X-ray diffractometry (XRD). All codendrimers exhibit smectic A mesomorphism. Besides, two compounds belonging to series I present uncommon mesophases originated by the incompatibility of the fluorinated and perhydrogenated chains. On the basis of the experimental results, a supramolecular model is proposed. AFM experiments on some of the compounds were also performed to investigate their surface aggregation behavior.

Introduction

Supramolecular organization originated by self-assembly processes represents one of the most thriving topics of research related to dendrimers.[1] The high number of functional groups that these molecules contain at their periphery allows, by means of a well selected functionalization, to design novel supramolecular architectures. This is of particular importance in the liquid crystal field, where the mesomorphic order is affected by subtle changes in the intra- and intermolecular interactions.[2] Many liquid crystal dendrimers contain mesogenic units attached covalently to the dendrimer core, but recently noncovalent interactions, especially the ionic linkage,[3] has attracted increasing interest due to the versatility and simplicity involved in the synthesis of these materials.

On the other hand, the introduction of fluorine in organic compounds can drastically affect their physical and chemical behavior, giving materials with interesting applications.[4] In the liquid crystal field, incorporation of fluorinated chains have promoted great attention because of their special properties such as lower viscosity, enhanced chemical, thermal, and mesomorphic stability, reduction of flexibility, and the possibility of introducing additional dipole moments.[5] The incompatibility of fluorocarbons with aliphatic hydrocarbons produces their segregation into distinct microdomains, and this

*To whom correspondence should be addressed. E-mail: jbarbera@unizar.es.

(1) (a) Astruc, D.; Boisselier, E.; Ornelas, C. *Chem. Rev.* **2010**, *110*, 1857–1959. (b) Vögtle, F.; Richardt, G.; Werner, N. *Dendrimer Chemistry*; Wiley-VCH: Weinheim, Germany, 2009.
(2) (a) Rosen, B. M.; Wilson, J. C.; Wilson, D. A.; Petarca, M.; Imam, M. R.; Percec, V. *Chem. Rev.* **2009**, *109*, 6275. (b) Marcos, M.; Martín-Rapún, R.; Omenat, A.; Serrano, J. L. *Chem. Soc. Rev.* **2007**, *36*, 1889. (c) Donnio, B.; Guillon, D. *Adv. Polym. Sci.* **2006**, *201*, 45.
(3) (a) Hernández-Ainsa, S.; Marcos, M.; Barberá, J.; Serrano, J. L. *Angew. Chem., Int. Ed.* **2010**, *49*, 1990–1994. (b) Mezzenga, R.; Ruokolainen, J.; Canilho, N.; Kasëmi, E.; Schlüter, D. A.; Lee, W. B.; Fredricksone, G. H. *Soft Matter* **2009**, *5*, 92–97. (c) Martín-Rapún, R.; Marcos, M.; Omenat, A.; Barberá, J.; Romero, P.; Serrano, J. L. *J. Am. Chem. Soc.* **2005**, *127*, 7397. (d) Binnemans, K. *Chem. Rev.* **2005**, *105*, 4148.
(4) (a) Zhang, W. *Chem. Rev.* **2009**, *109*, 749. (b) Gladysz, J. A.; Curran, D. P.; Horvath, I. T. *Handbook of Fluorous Chemistry*; Wiley-VCH: New York, 2004. (c) Caminade, A. M.; Turrin, C. O.; Sutra, P.; Majoral, J. P. *Curr. Opin. Colloid Interface Sci.* **2003**, *8*, 282. (d) Pitois, C.; Vestberg, R.; Rodlert, M.; Malmström, E.; Hult, A.; Lindgrem, M. *Opt. Mater.* **2002**, *21*, 499.
(5) (a) Hird, M. Chem. Soc. Rev. **2007**, *36*, 2070 and references therein. (b) Tomalia, D. A. *Nat. Mater.* **2003**, *2*, 711. (c) Johansson, G.; Percec, V.; Hungar, G.; Zhou, J. P. *Macromolecules* **1996**, *29*, 646.
(6) (a) Stipetic, A. I.; Goodby, J. W.; Hird, M.; Raoul, Y. M.; Gleeson, H. F. *Liq. Cryst.* **2006**, *33*, 819. (b) Cowling, S. J.; Hall, A. W.; Goodby, J. W.; Wang, Y.; Gleeson, H. F. *J. Mater. Chem.* **2006**, *16*, 2181. (c) Percec, V.; Glodde, M.; Johansson, G.; Balagurusamy, V. S. K.; Heiney, P. A. *Angew. Chem., Int. Ed.* **2003**, *42*, 4338. (d) Drzewinski, W.; Czuprymski, K.; Dabrowski, R.; Neubert, M. *Mol. Cryst. Liq. Cryst.* **1999**, *328*, 401.
(7) (a) Yamaguchi, A.; Uehara, N.; Yamamoto, J.; Yoshizawa, A. *Chem. Mater.* **2007**, *19*, 6445. (b) Yoshizawa, A.; Yamamoto, K.; Dewa, H.; Nishiyama, I.; Yamamoto, J.; Yokohama, H. *J. Mater. Chem.* **2003**, *13*, 172. (c) Kohlmeier, A.; Janietz, D. *Chem. Mater.* **2006**, 18. (d) Kölbel, M.; Beyersdorff, T.; Cheng, X. H.; Tschierske, C.; Kain, J.; Diele, S. *J. Am. Chem. Soc.* **2001**, *123*, 6809.

 Published on Web 07/23/2010

Scheme 1. Synthetic Route for Ionic Dendrimers: Series I and Series II[a]

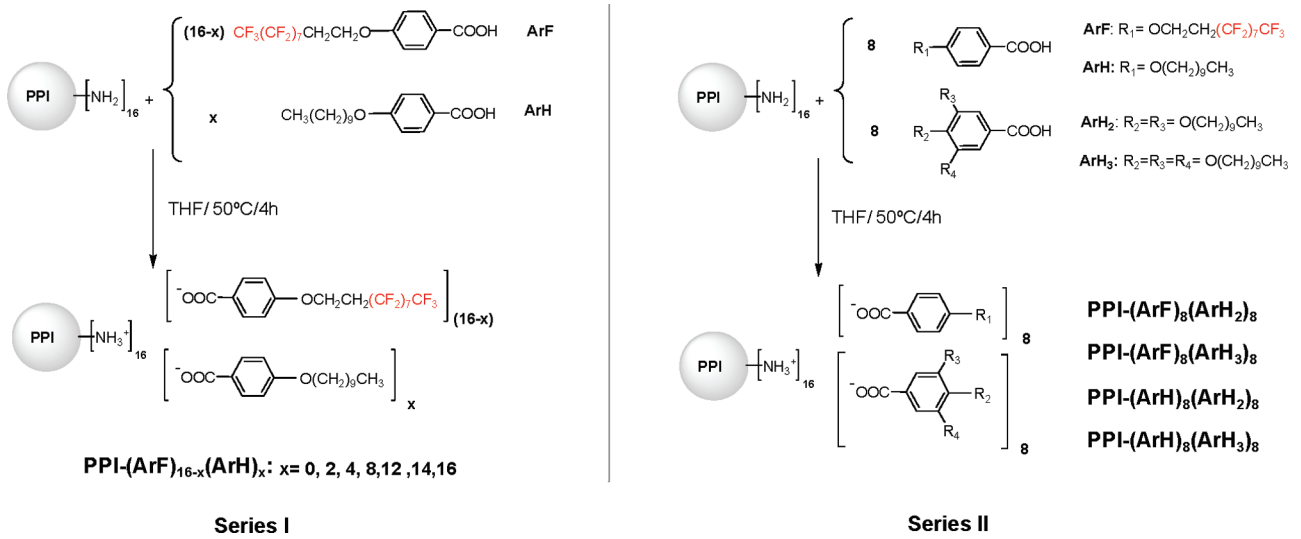

[a] IR and NMR spectroscopy, together with elemental analysis, reveal the correct formation of the ionic dendrimers (series I and II).

fact promotes the apparition of mesomorphic properties due to self-assembly of these different molecular units.[6] Some frustrated[7,3a] or modulated phases[8] have been found in these kind of systems.

Although liquid crystalline fluorinated aromatic dendrons have been broadly explored by Percec,[9,6c,2a] few examples involving dendrimers have been reported to date. In this way, Frey and co-workers[10] presented the synthesis and characterization of a series of four carbosilane dendrimers bearing 4, 12, 36, and 108 C_6F_{13} end groups which exhibited liquid crystal properties depending on the dendrimer generation. Tschierske and co-workers[11] reported the stabilization of the liquid crystal behavior in the first generation of a pentaerythritol tetrabenzoate dendrimer when fluorinated chains are incorporated in the dendrimer structure. Our group has previously described the mesomorphic behavior of a series of ionic dendrimers derived from PPI and PAMAM functionalized with a semifluorinated carboxylic acid.[12] We have recently reported the apparition of a frustrated smectic mesophase when the third generation PPI dendrimer is ionically substituted with perhydrogenated and semifluorinated chains in different proportions. In this case the competition of both substituents to control the supramolecular organization of the molecules produces particular mesomorphic properties.[3a]

On the other hand, we observed that the introduction of three decyloxy units in a rigid moiety, namely, benzoic acid, produces columnar phases by the ionic junction of this aromatic acid to the surface of PPI dendrimers of the first five generations.[13]

In order to investigate the influence that the incorporation of a rigid moiety to the structure of the fluorinated acids exercises in the liquid crystal properties of these dendrimers, we present here the mesomorphic properties of two series of ionic codendrimers (Scheme 1). The first series is produced by the ionic attachment of 4-decyloxybenzoic acid and 4-(1H,1H,2H,2H)-perfluorodecyloxybenzoic acid in different proportions to the poly(propyleneimine) dendrimer (PPI) of the third generation (series I). The second series is constituted by four ionic dendrimers containing eight units of 3,4-didecyloxybenzoic acid or 3,4,5-tridecyloxybenzoic acid and eight units of 4-decyloxybenzoic acid or 4-(1H,1H,2H,2H)-perfluorodecyloxybenzoic acid (series II). This series has been designed to analyze the influence of the tail chain contents of the aromatic acid in the mesomorphic properties. Apart from thoroughly investigating their mesomorphic properties, some materials have been studied by atomic force microscopy (AFM) to investigate their surface aggregation tendency.

Materials and Methods

PPI-$(NH_2)_{16}$ dendrimer was purchased from SyMO-Chem BV (Eindhoven, The Netherlands). Methyl (3,4,5-trihydroxy)benzoate, ethyl (3,4-dihydroxy)benzoate, 4-decyloxybenzoic acid, and 1-bromodecane were purchased from Aldrich. 1H,1H,2H,2H-Perfluorodecanol was purchased from Lancaster. 4-Decyloxybenzoic acid was recrystallized from ethanol before use. The rest of reagents were used as received.

The infrared spectra of all the compounds were obtained with a Nicolet Avatar 360 FTIR spectrophotometer in the 400−4000 cm^{-1} spectral range using KBr pellets and NaCl cells. ^1H NMR was performed on a Bruker AVANCE 400 spectrometer

(8) (a) Lee, W. K.; Kim, K. N.; Achard, M. F.; Jin, J. I. *J. Mater.Chem.* **2006**, *16*, 2289. (b) Nyugen, H. T.; Sigaud, G.; Achard, M. F.; Hardouin, F.; Twieg, R. J.; Betterton, K. *Liq. Cryst.* **1991**, *10*, 389.
(9) (a) Dukeson, D. R.; Ungar, G.; Balagurusamy, V. S. K.; Percec, V.; Johansson, G. A.; Glodde, M. *J. Am. Chem. Soc.* **2003**, *125*, 15974. (b) Percec, V.; Glodde, M.; Bera, T. K.; Miura, Y.; Shiyanovskaya, I.; Singer, K. D.; Balagurusamy, V. S. K.; Heiney, P. A.; Schnell, I.; Rapp, A.; Spiess, H.-W.; Hudson, S. D.; Duan, H. *Nature* **2002**, *419*, 384.
(10) (a) Lorenz, K.; Frey, H.; Stühn, B.; Mülhaupt, R. *Macromolecules* **1997**, *30*, 6860. (b) Stark, B.; Stühn, B.; Frey, H.; Lach, C.; Lorenz, K.; Frick, B. *Macromolecules* **1998**, *31*, 5415. (c) Stark, B.; Lach, C.; Frey, H.; Stühn, B. *Macromol. Symp.* **1999**, *146*, 33.
(11) (a) Pegenau, A.; Cheng, X. H.; Tschierske, C.; Göring, P.; Diele, S. *New J. Chem.* **1999**, *23*, 465. (b) Cheng, X. H.; Diele, S.; Tschierscke, C. *Angew. Chem., Int. Ed.* **2000**, *39*, 592.
(12) Martín-Rapún, R.; Marcos, M.; Omenat, A.; Serrano, J. L.; Taffin de Givenchy, E.; Guittard, F. *Liq. Cryst.* **2007**, *34*, 395.
(13) Marcos, M.; Martín-Rapún, R.; Omenat, A.; Barberá, J.; Serrano, J. L. *Chem. Mater.* **2006**, *18*, 1206.

and on a Bruker AVANCE 300 spectrometer. ^{13}C NMR was performed on a Bruker AVANCE 400 spectrometer operating at 100 MHz. ^{19}F-NMR experiments were carried out on a Bruker AVANCE 400 spectrometer operating at 376 MHz and on a Bruker AVANCE 300 spectrometer operating at 282 MHz.

Mesogenic behavior and transition temperatures were determined using an Olympus BH-2 polarizing microscope equipped with a Linkam TMS91 hot stage and a CS196 hot-stage central processor. DSC-MDSC TA Instruments 2910, Q-1000 and Q-2000 equipments were used to execute differential scanning calorimetry (DSC) experiments. Samples were sealed in aluminum pans, and a scanning rate of 10 °C/min under a nitrogen atmosphere was used. Three cycles were carried out. The first cycle was performed up to temperatures 50 degrees below the isotropization process to avoid decomposition of the materials. The second and third cycles were performed until the isotropization temperature. Temperatures were taken at the maximum of the transition peaks in the first heating scan. Thermogravimetric analysis (TGA) was performed using a TA Instruments STD 2960 simultaneous TGA-DTA at a rate of 10 °C min^{-1} under argon atmosphere.

The XRD experiments were performed in a pinhole camera (Anton-Paar) operating with a point-focused Ni-filtered Cu−Kα beam with a cross section of 1 mm^2. Lindemann glass capillaries with 1 mm diameter were used to contain the sample. When necessary, a variable-temperature oven was used to heat the sample. The capillary axis is perpendicular to the X-ray beam and the pattern is collected on flat photographic film perpendicular to the X-ray beam. Bragg's law was used to obtain the spacings.

The AFM experiments were performed by using a multimode extended microscope with Nanoscope IV electronics from Veeco. The AFM tip used was made of silicon with a resonance frequency of 265 kHz and a force constant of 40 N m^{1-}. The scanning rate was 1 Hz, and the amplitude set point was lower than 1 V. All images were obtained at room temperature and in ambient atmosphere using the tapping mode. Samples were prepared by solvent (CF_3CH_2OH) casting on freshly cleaved mica at ambient conditions.

Results and Discussion

Synthesis and Characterization. Ionic codendrimers (series I and II) were synthesized as follows (Scheme 1). Amine-terminated PPI dendrimer of third generation was added to a solution of the corresponding acids in dry tetrahydrofuran (THF), in the stoichiometry necessary to functionalize all amine groups of the periphery. The mixture was stirred for 4 h at 50 °C, and the solvent was evaporated under vacuum to obtain the ionic compound.

FT-IR Study. The carbonyl stretching absorption 1685−1670 cm^{-1} band corresponding to fluorinated (ArF) and nonfluorinated aromatic acids (ArH, ArH_2, ArH_3) disappeared, and a new band corresponding to the asymmetric stretching absortion of carboxylate group 1550−1540 cm^{-1} appeared in ionic codendrimers (Figure 1).

NMR Study. Ionic dendrimers were studied by ^1H NMR spectroscopy. Samples consisting of each codendrimer were dissolved in DMSO-d_6 and heated (90 °C) when containing fluorinated acid. The appearance of the signal at ∼2.62 ppm corresponding to [−C$\underline{H}_2$−NH_3^+] and the absence of signal at 2.52 ppm related to

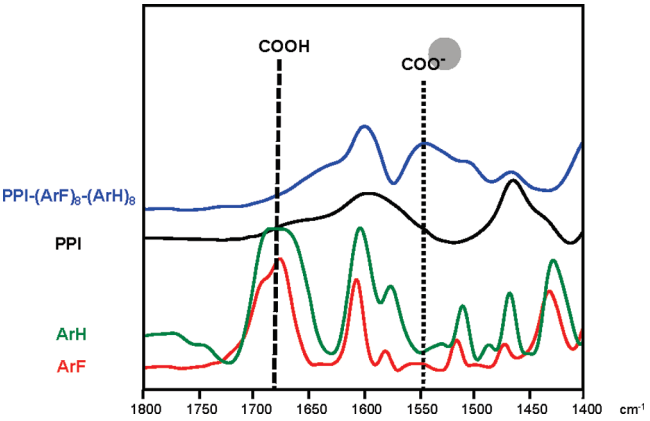

Figure 1. FT-IR in the range of carbonyl group for PPI (black), ArH (green), ArF (red), and PPI-$(ArF)_8$-$(ArH)_8$ (blue).

[−C$\underline{H}_2$−NH_2] of PPI[14] confirmed the full formation of the salts (Figure 2a).

Experimental percentage of each acid conforming the codendrimers of series I and II was examined by ^1H NMR. In series I, signals corresponding to the protons of the methylene group situated α to the oxygen (ArOC$\underline{H}_2$) in 4-decyloxybenzoate and 4-(1H,1H,2H,2H-perfluorodecyloxy)benzoate, which appear at ∼4.05 ppm and ∼4.40 ppm, respectively, were integrated. As it was expected for the synthetic employed method, experimental and theoretical integrated values agree (see Figure 2b and Figure S4 in the Supporting Information). It is important to highlight that the obtained ratio is an average, and the actual distribution is statistical because these compounds have been prepared at random. Moreover, their ionic nature prevents the use of techniques such as gel permeation chromatography (GPC) or matrix-asssisted laser desorption ionization-time-of-flight (MALDI-TOF) mass spectrometry to precisely determine the exact composition of each moiety in the codendrimer. However, the distribution is expected to be centered on the desired composition as supported by GPC measurements in some series of covalent codendrimers previously reported by us which were also prepared at random.[15]

Thermal and Mesomorphic Properties. The phase behavior of the codendrimers was analyzed by polarizing optical microscopy (POM) and differential scanning calorimetry (DSC). The mesophases and transition temperatures of the different compounds are gathered in Figure 3. No accurate enthalpy value data can be given due to the small area and broadness of the peaks. Compounds begin to lose weight upon transition to the isotropic liquid as observed by thermogravimetric analysis (TGA). In fact, 5% of the weight is lost at around 200 °C (see the Supporting Information). Therefore, the first cycle in

(14) (a) Tsiourvas, D.; Felekis, T.; Sideratou, Z.; Paleos, C. *Liq. Cryst.* **2004**, *31*, 739. (b) Baars, M. W. P. L.; Karlsson, A. J.; Sorokin, V.; de Waal, B. F.W.; Meijer, E. W. *Angew. Chem.* **2000**, *112*, 4432.
(15) (a) Serrano, J. L.; Marcos, M.; Martín-Rapún, R.; González, M.; Barberá, J. *Chem. Mater.* **2003**, *15*, 3866. (b) Rueff, J.-M.; Barberá, J.; Donnio, B.; Guillon, D.; Marcos, M.; Serrano, J. L. *Macromolecules* **2003**, *36*, 8368. (c) Martín-Rapún, R.; Marcos, M.; Omenat, A.; Serrano, J. L.; Luckhurst, G. R.; Mainal, A. *Chem. Mater.* **2004**, *16*, 4969.

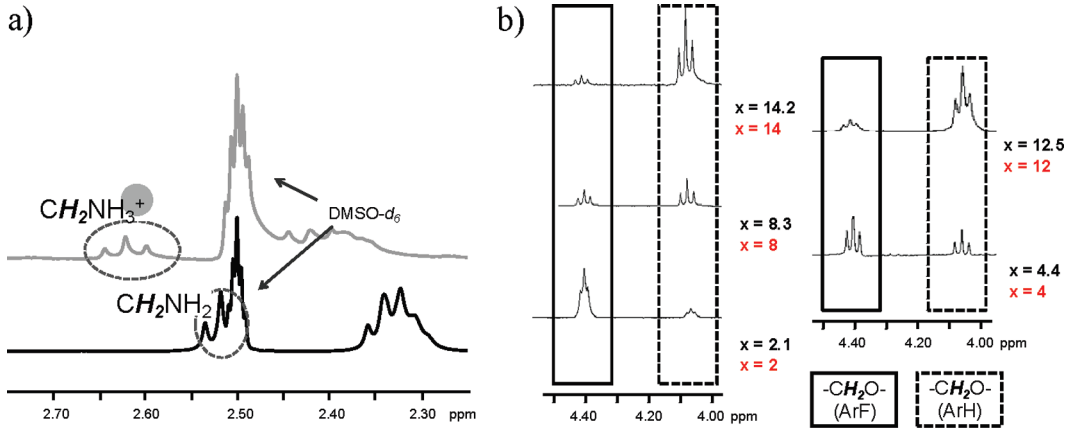

Figure 2. (a) ^{1}H NMR of PPI and PPI-$(ArF)_2(ArH)_{14}$ in the range of the protons corresponding to $C\underline{H_2}NH_2$ and $C\underline{H_2}NH_3^+$, respectively. (b) Experimental (black) and theoretical (red) composition determined by the integration of signals corresponding to the methylene protons $-OC\underline{H_2}-$ from ArF and ArH of PPI-$(ArF)_{16-x}(ArH)_x$ (series I) in ^{1}H NMR experiments.

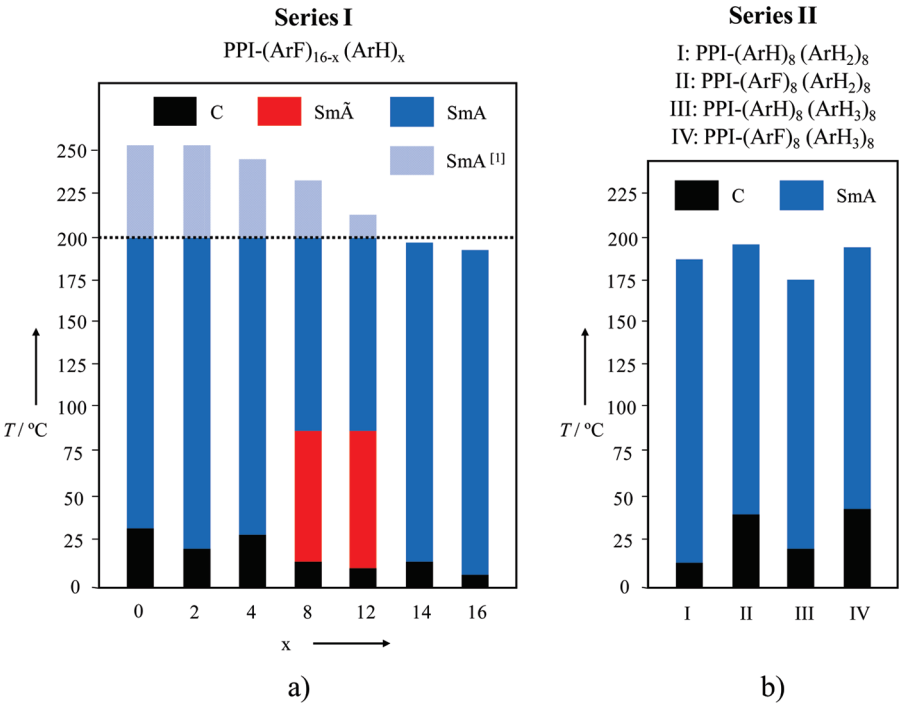

Figure 3. Mesomorphic behavior of the compounds of (a) series I (PPI-$(ArF)_{16-x}$ $(ArH)_x$), (b) series II (I, PPI-$(ArH)_8(ArH_2)_8$; II, PPI-$(ArF)_8(ArH_2)_8$; III, PPI-$(ArH)_8(ArH_3)_8$; IV, PPI-$(ArF)_8(ArH_3)_8$). C, crystalline phase; SmÃ, modulated phase. The SmÃ−SmA transition temperatures were deduced from X-ray diffraction measurements. SmA, smectic A phase. SmA[1] phase coexisting with the partially decomposed material. *Y* axis: temperature (°C). *X* axis: (a) average number of units of 4-decyloxybenzoic acid (ArH) that contains the codendrimer and (b) compound notation.

differential scanning calorimetry experiments was carried out up to a temperature below the initial decomposition temperature, and melting temperature data were taken from this first heating cycle. The isotropization temperatures were taken from POM observations. All codendrimers present liquid crystalline behavior and self-assemble in a smectic A mesophase, which was clearly identified by the fan-shaped and batônnets textures observed in POM (Figure 4). Moreover, as it will be discussed below, an additional low-temperature mesophase (SmÃ) has been found for two codendrimers of series I (x = 8, 12).

Two facts have been analyzed in relation to the thermal behavior of these compounds: the nature of the substituent attached to the dendrimer (fluorinated or perhydrogenated) and the variation in the number of chains attached to the aromatic core of the perhydrogenated acid (ArH, ArH_2, ArH_3).

Compounds of series I present larger mesomorphic temperature ranges when the contents in fluorinated moieties (ArF) increases (Figure 3a). Similarly, higher clearing temperatures are observed in series II upon increasing the fluorine contents (Figure 3b). Thus, as expected, fluorinated chains stabilize the liquid crystalline state.[16]

The number of chains attached to the aromatic core in the perhydrogenated acid exercises a marked effect on the isotropization temperature. In this way, PPI-$(ArF)_8(ArH)_8$ (series I) exhibits a higher clearing point than PPI-$(ArF)_8$-$(ArH_2)_8$ and PPI-$(ArF)_8(ArH_3)_8$ (series II). When no

(16) Eaton, D. F.; Smart, B. E. *J. Am. Chem. Soc.* **1990**, *112*, 2821.

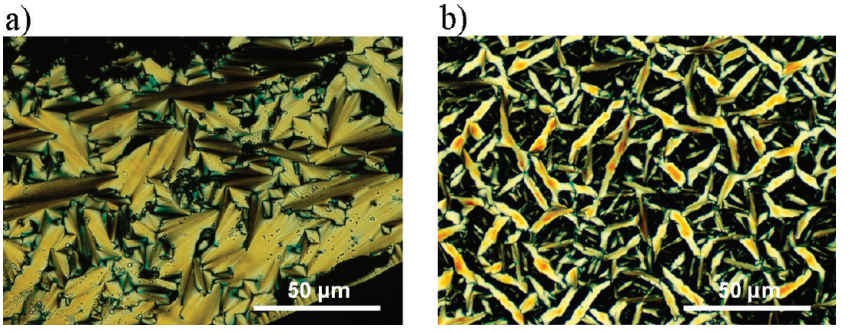

Figure 4. POM texture observed in the cooling process: (a) PPI-$(ArF)_8(ArH)_8$ (series I) at 188 °C and (b) PPI-$(ArH)_8(ArH_2)_8$ (series II) at 161 °C.

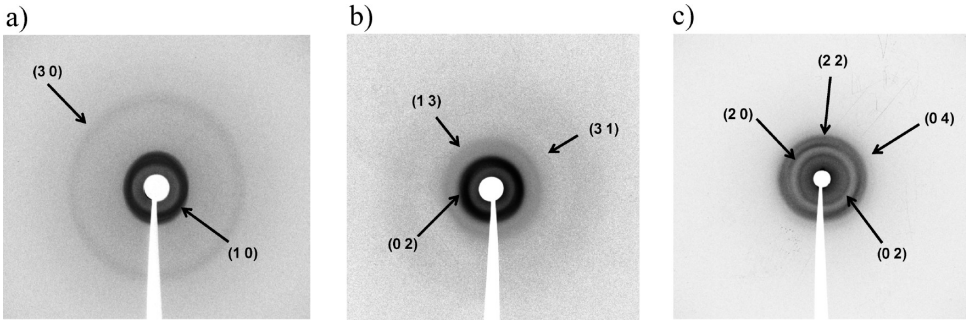

Figure 5. Small-angle XRD patterns and indexation of (a) PPI-$(ArF)_{14}(ArH)_2$ in the SmA phase at 110 °C, (b) PPI-$(ArF)_8(ArH)_8$, and (c) PPI-$(ArF)_4(ArH)_{12}$ in the SmÃ at room temperature. The (0 4) reflection in part c is very weak, but it is visible in the long-exposure-time patterns (see Figure S5 in the Supporting Information).

fluorinated moiety is contained in the dendrimer, a progressive decrease in the isotropization temperature is observed upon increasing the number of decyloxy chains (compare PPI-$(ArH)_{16}$ (x = 16), PPI-$(ArH)_8(ArH_2)_8$ (compound I) and PPI-$(ArH)_8(ArH_3)_8$ (compound III)).

XRD Study. The diffraction patterns of the materials confirmed that all the compounds display SmA mesomorphism. The patterns present a diffuse halo in the wide angle region, corresponding to the correlations between the conformationally disordered perhydrogenated or semifluorinated chains, and one or two sharp maxima in the small angle region. The diffuse halo shifts from higher angles (interchain distance) for the perhydrogenated chains close to 4.5 Å to lower angles (interchain distance close to 5.4 Å) for the semifluorinated chains. For compounds containing a high percentage of the perhydrogenated chains, only a single peak is observed in this region, whereas two sharp maxima with reciprocal spacing in the relationship (1:3) are observed for compounds containing a high percentage of the fluorinated moiety (ArF) (Figure 5a). These sharp maxima evidence a long-range lamellar packing of molecules adopting an approximately cylindrical shape. The absence of the 2nd order reflection in the smectic phases of these fluorinated compounds is probably the consequence of the form factor of the molecules, due to the presence of the dense fluorinated chains, which are expected to project a maximum in the electronic density on the director. The extra contrast in electronic density between the different component regions of the molecule can account for the weakening of the even diffraction peak and the dominant intensity of the odd peaks. Fluorocarbon chains are incompatible with the dendrimer core and the benzene rings, and consequently lamellar arrangements can be expected as a result of segregation between the different regions of the molecule. When applying Bragg's law to the low angle maxima, the values of the layer thickness in the SmA mesophase for all the dendrimers are obtained (Table 1). The layer thickness d is the parameter characteristic of the layer structure and is approximately equal to the length of one single molecule (Figure 6a).

Table 1. Layer Spacing and Rectangular Lattice Constants Determined by X-ray Diffraction for the Compounds at the Indicated Temperature

series	codendrimer	mesophase	T^a/°C	structural parameters (Å)[a]
I	PPI-$(ArF)_{16}$	SmA	115	d = 37.6
I	PPI-$(ArF)_{14}(ArH)_2$	SmA	110	d = 37.7
I	PPI-$(ArF)_{12}(ArH)_4$	SmA	100	d = 37.9
I	PPI-$(ArF)_8(ArH)_8$	SmÃ	rt	a = 68.0, b = 94.0
I	PPI-$(ArF)_8(ArH)_8$	SmA	100	d = 36.5
I	PPI-$(ArF)_4(ArH)_{12}$	SmÃ	rt	a = 66.5, b = 94.5
I	PPI-$(ArF)_4(ArH)_{12}$	SmA	110	d = 34.0
I	PPI-$(ArF)_2(ArH)_{14}$	SmA	110	d = 31.7
I	PPI- $(ArH)_{16}$	SmA	110	d = 30.8
II	PPI-$(ArH)_8(ArH_2)_8$	SmA	100	d = 32.9
II	PPI-$(ArF)_8(ArH_2)_8$	SmA	100	d = 35.2
II	PPI-$(ArH)_8(ArH_3)_8$	SmA	100	d = 30.8
II	PPI-$(ArF)_8(ArH_3)_8$	SmA	100	d = 33.3

[a] d = Layer spacing of the smectic A phase. a, b = rectangular lattice constants of the modulated smectic phase.

The spacing layer increases with the contents of fluorinated moiety (ArF) for compounds of series I. Besides, when comparing the layer spacing of the condendrimers containing 50% of fluorinated moiety (ArF) a decrease is observed when the number of decyloxy chains attached to

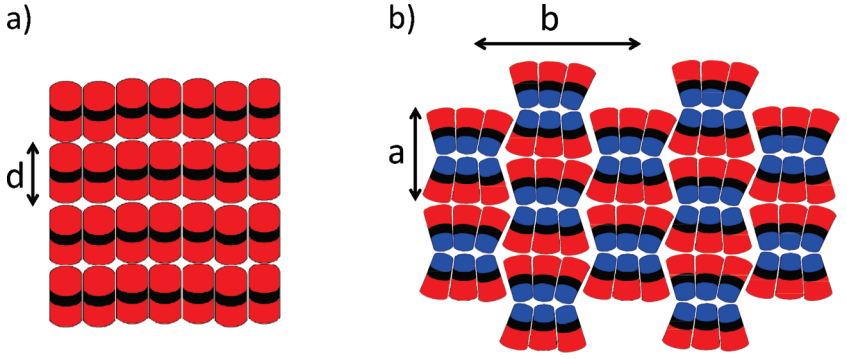

Figure 6. Schematic representation of proposed molecular organization of (a) PPI-$(ArF)_{16}$ in the SmA phase, (b) PPI-$(ArF)_8(ArH)_8$ in the SmÃ phase. Key: perhydrogenated moiety in blue; semifluorinated moiety in red; PPI matrix in black. *d*: spacing layer in the SmA phase. *a*, *b*: parameters of the SmÃ phase.

the perhydrogenated moiety grows. Thus, the spacing layers observed for PPI-$(ArF)_8$-$(ArH)_8$, PPI-$(ArF)_8$-$(ArH_2)_8$, and PPI-$(ArF)_8$-$(ArH_3)_8$ are 36.5, 35.2, and 33.3 Å, respectively.

In addition to the X-ray patterns characteristics of the SmA phase, codendrimers PPI-$(ArF)_8(ArH)_8$ and PPI-$(ArF)_4(ArH)_{12}$ belonging to series I present a different diffraction pattern when studied at lower temperatures (Figure 5b,c and Figure S5 in the Supporting Information). The patterns consist of three (for PPI-$(ArF)_8(ArH)_8$) or four (for PPI-$(ArF)_4(ArH)_{12}$) sharp rings in the small-angle region and a diffuse halo in the wide-angle region. The ratio between the spacings corresponding to the small-angle region angle does not correspond to a simple lamellar structure. Instead, the found reflections fit a centered rectangular lattice (see the Supporting Information). To interpret this result the following facts have to be taken into account: (i) in the case of PPI-$(ArF)_4(ArH)_{12}$ a maximum at 33.2 Å is observed that is close to the layer spacing found for the SmA phase of this compound at higher temperatures (Table 1); (ii) on the other hand, no maximum is observed for PPI-$(ArF)_8(ArH)_8$ with a value similar to the layer spacing measured for its SmA phase; (iii) the rectangular lattice constants deduced from the X-ray patterns are a = 68 Å, b = 94 Å for PPI-$(ArF)_8(ArH)_8$, and a = 66.5 Å, b = 94.5 Å for PPI-$(ArF)_4(ArH)_{12}$; (iv) in both cases, a is roughly twice the value of the SmA layer spacing (Table 1). All these features are consistent with a mesophase with a ribbonlike structure, namely, a modulated smectic A phase (SmÃ). Modulated smectic mesophases or antiphases have been described for a number of low-molecular-weight mesogens carrying terminal polar groups[17] and have also been reported for mesogens with fluorinated terminal chains.[8] Our group has described this type of mesophase for some codendrimers containing laterally attached mesogenic units[18] or combining laterally and terminally attached mesogenic units.[15c]

We have recently reported the existence of a frustated smectic A (SmA^+) phase for compounds which resemble those of series I but deprived of the benzene ring.[3a] In the present paper, the apparition of another kind of disrupted mesophase for compounds of series I when the percentage of ArH and ArF is the same (x = 4, 8) as for the previously reported analogous aliphatic codendrimers displaying the SmA^+ phase is noticeable. Here, compounds exhibiting the modulated SmÃ phase (x = 4, 8) contain less than 70% of the majority moiety (calculated in cross-sectional area) (see the Supporting Information). The chemical incompatibility[19] and differences in cross sectional area between the fluorinated and perhydrogenated chains (0.28 nm^2 for fluorinated chains and 0.18 nm^2 for aliphatic chains)[20] precludes the arrangement of both types of moiety together in the same layer and, therefore, nanosegregation most probably takes place in each layer into hydrocarbon and fluorocarbon sublayers. This layer structure is defined by parameter a, which is approximately double the length of one single molecule (Figure 6b). The layers of the resulting mesophase exhibit undulation in a direction perpendicular to the layer normal as a consequence of the dissymmetry originated by the nanosegregation of both moieties. The formation of the two-dimensional rectangular face-centered lattice characteristic of the SmÃ phase can be explained by the mismatch between the space filling and cross-section requirements of the fluorocarbon and hydrocarbon chains. As a consequence of this mismatch, the molecules are expected to adopt the shape of a conical frustrum. The differences in cross section between the larger base (S_1) and the smaller base (S_2) of the conical frustrum (Figure S6 in the Supporting Information) generate a strain that is relieved by the layers breaking into ribbons arranged parallel to the layer planes and organized in a rectangular lattice (Figure 6b). The doubling of the periodicity along the director (rectangular lattice constant a compared to smectic layer spacing d) corresponds to the distance between two consecutive, equally oriented molecules. Taking into account parameter b and the length of each molecule (approximately equal to the d value obtained in the SmA phase), it is possible to estimate that the

(17) Demus, D.; Goodby, J. W.; Gray, G. W.; Spiess, H.-W.; Vill, V. *Handbook of Liquid Crystals*; Wiley-VCH: Weinheim, Germany, 1998; Vol. *1*, Chapter 3.
(18) Barberá, J.; Giménez, R.; Marcos, M.; Serrano, J. L. *Liq. Cryst.* **2002**, *29*, 309.
(19) Krafft, M. P.; Riess, J. G. *Chem. Rev.* **2009**, *109*, 1714.
(20) Lose, D.; Diele, S.; Pelz, G.; Dietzmann, E.; Weissflog, W. *Liq. Cryst.* **1998**, *24*, 707.

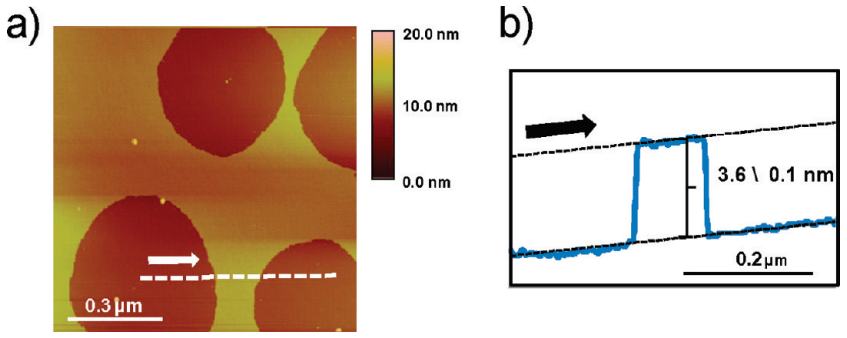

Figure 7. AFM images of PPI-$(ArF)_8(ArH)_8$: (a) topographic image and (b) cross section.

mismatch takes place between groups of about three molecules along the *b* direction (see the Supporting Information).

In fair agreement with the results for the analogous aliphatic codendrimers,[3a] the junction of different nature (perhydrogenated and semifluorinated) chains in the same molecule generates a competition to dominate the supramolecular organization. In contrast, a large predominance of one type of chain, either hydrocarbon or fluorocarbon, makes it impossible to arrange each type of moiety in different sublayers and, therefore, a simple layer structure (Figure 6a) is the most stable one because the majority chain is able to accommodate the minority one, although it implies mixing fluorinated and perhydrogenated chains. Indeed, careful X-ray analysis of all the compounds at variable temperatures rules out the presence of the modulated smectic phase in any compound apart from PPI-$(ArF)_8(ArH)_8$ and PPI-$(ArF)_4$-$(ArH)_{12}$. In this case, the molecules have a tendency to maximize their entropy, as opposed to the case of the molecules displaying the SmÃ phase where the amphipatic forces and geometrical constraints determine a more ordered packing.

It is interesting to note that the low-temperature SmÃ mesophase evolves to a more disordered SmA at higher temperatures, probably because the increasing temperature facilitates the mixture of both moieties.

At first sight, it could be expected the same phenomena for compounds of series II containing fluorinated moieties, because they contain the same number of acids with either aliphatic (ArH_2 or ArH_3) or fluorinated (ArF) chains. However, the higher number of perhydrogenated chains in the aromatic acids compared to series I make these compounds of series II able to overcome the disruption effect caused by the fluorinated chains.

AFM Studies. AFM was used to examine the self-assembly process on mica of these aromatic dendrimers at room temperature. The samples were prepared by drop casting solutions in CF_3CH_2OH of the samples (0.5%, wt%) on freshly cleaved mica. As it can be observed in Figure 7, PPI-$(ArF)_8(ArH)_8$ organized in layers with a height corresponding to the length of a single molecule. Thus, the same tendency as for the previously reported PPI dendrimers functionalized with aliphatic perhydrogenated and semifluorinated acids was observed.[3a] Thus, there is a relationship between the supramolecular organization that occurs in the mesomorphic state and the layer order exhibited when these compounds are allowed to self-assemble on a substrate, in this case mica.

Conclusions

Ionic grafting has demonstrated a great ability to promote liquid crystalline properties when aromatic acids substituted with fluorinated or perhydrogenated chains are attached to the poly(propyleneimine) (PPI) dendrimer of the third generation. Most of the liquid crystalline compounds exhibit smectic A mesomorphism. However, the incompatibility between fluorinated and perhydrogenated chains plays a crucial role in the supramolecular organization and produces uncommon mesophases, namely, modulated smectic phases, when both moieties are introduced in similar proportions. Interestingly, AFM studies reveal the flattened organization that these liquid crystalline codendrimers present on a surface.

Acknowledgment. This work was supported by the MICINN, Spain, under Project CTQ2009-09030, and FEDER funding EU, by seventh FP-THE PEOPLE PROGRAMME, The Marie Curie Actions, ITN, Grant No. 215884-2, and by the Gobierno de Aragón (Project PI109/09, Research Group E04). S.H.-A. thanks the MICINN (Spain) for a FPU grant.

Supporting Information Available: Additional details about the synthesis, characterization, NMR spectra, TGA, and X-ray data of the materials (PDF). This material is available free of charge via the Internet at http://pubs.acs.org.